ORIGINAL ARTICLE

Biogeochemical conditions determine virulence of black band disease in corals

Martin S Glas[1], Yui Sato[2,3], Karin E Ulstrup[4] and David G Bourne[2]

[1]*Max Planck Institute for Marine Microbiology, Microsensor Group, Bremen, Bremen, Germany;* [2]*Centre of Marine Microbiology and Genetics, Australian Institute of Marine Science, PMB 3, Townsville, Queensland, Australia;* [3]*ARC Centre of Excellence for Coral Reef Studies and School of Marine and Tropical Biology, James Cook University, and AIMS@JCU, Townsville, Queensland, Australia and* [4]*DHI Water & Environment, West Perth, Western Australia, Australia*

The microenvironmental dynamics of the microbial mat of black band disease (BBD) and its less virulent precursor, cyanobacterial patch (CP), were extensively profiled using microsensors under different light intensities with respect to O_2, pH and H_2S. BBD mats exhibited vertical stratification into an upper phototrophic and lower anoxic and sulphidic zone. At the progression front of BBD lesions, high sulphide levels up to 4977 μM were measured in darkness along with lower than ambient levels of pH (7.43 ± 0.20). At the base of the coral–BBD microbial mat, conditions were hypoxic or anoxic depending on light intensity exposure. In contrast, CP mats did not exhibit strong microchemical stratification with mostly supersaturated oxygen conditions throughout the mats at all light intensities and with levels of pH generally higher than in BBD. Two of three replicate CP mats were devoid of sulphide, while the third replicate showed only low levels of sulphide (up to 42 μM) present in darkness and at intermediate light levels. The level of oxygenation and sulphide correlated well with lesion migration rates, that is virulence of the mats, which were greater in BBD than in CP. The results suggest that biogeochemical microgradients of BBD shaped by the complex microbial community, rather than a defined pathogen, are the major trigger for high virulence and the associated derived coral mortality of this disease.
The ISME Journal (2012) **6**, 1526–1534; doi:10.1038/ismej.2012.2; published online 9 February 2012
Subject Category: microbe–microbe and microbe–host interactions
Keywords: BBD; CP; pathogen; microsensor; anoxia; sulphide

Introduction

Black band disease (BBD) is a highly virulent coral disease that affects scleractinian corals, the major reef builders in tropical reef ecosystems around the world (Sutherland *et al.*, 2004). It manifests as a complex microbial mat that migrates over coral tissue, resulting in lysis and necrosis of the underlying coral tissue, leaving bare coral skeleton behind (Richardson, 2004). Despite being first identified in 1973 (Antonius, 1973), the aetiology and underlying mechanisms of pathogenesis and pathogenicity of BBD remain unresolved, as no primary pathogen has been identified and various causes for the disease's high virulence are still debated.

BBD comprises a complex microbial community including phototrophic cyanobacteria, sulphate-reducing bacteria (SRB), sulphide-oxidizing bacteria and other heterotrophic bacteria (Cooney *et al.*, 2002; Frias-Lopez *et al.*, 2004; Barneah *et al.*, 2007; Voss *et al.*, 2007; Sekar *et al.*, 2008; Sato *et al.*, 2010). The BBD lesion therefore closely resembles that of other complex microbial mats, as suggested by Carlton and Richardson (1995), including hypersaline mats, which are vertically stratified into an upper phototrophic zone and a lower anoxic-sulphidic zone (Jonkers *et al.*, 2003; Dupraz *et al.*, 2004, 2009; Ludwig *et al.*, 2005; Dillon *et al.*, 2009). The stratification in hypersaline mats is mainly driven by gliding filamentous members (cyanobacteria, *Beggiatoa* sp.) that are highly motile and exhibit active diurnal migration (Fourcans *et al.*, 2006; Hinck *et al.*, 2007; Dillon *et al.*, 2009). The vertical orientation of functional groups within hypersaline mats results in the development of pronounced biogeochemical microgradients (e.g., O_2, light, pH, sulphate and sulphide), reciprocally influenced by and influencing their environment. Such conditions enable tight spatial coupling of matter cycling, further driving development of functionally differentiated, stratified communities. Similar modulations of biogeochemical microgradients in BBD lesions are likely (Carlton and Richardson, 1995)

and may be an important trigger for high virulence at the base of the mat (coral–microbial mat interphase), where healthy tissue, necrosing tissue and the microbial consortium interact.

Biogeochemical conditions at the base of the BBD mat are typically hypoxic or anoxic with high concentrations of sulphide lethal to the underlying coral tissue. Such detrimental biogeochemical conditions established within and at the base of the mat have previously been suggested as virulence factors for BBD (Richardson et al., 1997). Yet, sulphide estimations within the microbial mat of BBD have focused on microsensor measurements of the S^{2-} fraction only, without taking pH variations within the mat into account (Carlton and Richardson, 1995). Importantly, the dissociation of the three sulphide species in seawater (H_2S, HS^- and S^{2-}) integrally depends on pH (Millero and Hershey, 1989) and the attained results therefore do not quantify total sulphide. Accurate measurements of the spatio-temporal dynamics of total sulphide is the key to understanding the onset and aetiology of BBD, as toxicity estimates for the coral tissue depend on the levels of total sulphide present (Vismann, 1991; Bagarinao, 1992; Richardson et al., 1997).

An outbreak of BBD and an earlier less-virulent stage of the disease, termed 'cyanobacterial patch' (CP), has been documented on Montipora coral species around Orpheus Island, within the Great Barrier Reef Marine Park (Sato et al., 2009, 2010). Transitions of CP-like lesions into developed BBD have also been observed on Indonesian reefs (B Willis, personal communication). In the field, BBD lesions develop from CP approximately 62 days following the onset of the CP lesion (Sato et al., 2010). Shifts in the microbial community structure as CP transitioned into BBD (Glas et al., 2010; Sato et al., 2010) included increases in sulphate-reducing bacterial (SRB) populations, namely Desulfovibrio sp. (Bourne et al., 2011). This disease outbreak around Orpheus Island also provided the opportunity to examine biogeochemical microgradients within the microbial mats, and the role microenvironmental conditions play in the virulence of BBD as well as the onset of BBD from CP.

To investigate if the high virulence of BBD is driven by the dynamic microenvironmental conditions within and at the base of the mat, we extensively profiled coral fragments infected with BBD and CP under controlled laboratory conditions with O_2, pH and H_2S (measuring the dissolved H_2S fraction) microsensors. The microsensor measurements were complemented with molecular quantification of sulphate reducers within the mat. The main aim of this study was therefore to further our understanding of virulence of CP and BBD by determining the spatio-temporal dynamics of pH, total sulphide and oxygen within and at the base of CP and BBD microbial mats and relate these results to the typical fast directional migration (virulence) of the corresponding lesions.

Materials and methods

Sampling and culturing
Samples of the scleractinian coral Montipora hispida infected with either CP or BBD ($n = 3$ colonies each, labelled as BBD no. 1–3 and CP no. 1–3) were collected in March 2010, using a hammer and chisel along the northeast coast of Pelorus Island (18°32′S, 146°30′E; central region of the Great Barrier Reef Marine Park, east coast of Australia), at depths of 3.5–4.5 m (for a detailed description of the study site, see Sato et al., 2009). Coral fragments infected with lesions of CP or BBD were carefully placed in separate 70-l cooling boxes containing ambient seawater, and immediately transported to the Australian Institute of Marine Science in Townsville. Samples were maintained in an indoor aquarium facility at 26 °C to avoid thermally induced transition of CP into BBD due to prevalent high summer temperatures (Glas et al., 2010). The facility provided a flow of freshly filtered seawater (3 cm s^{-1}) and light intensities of ~100 μmol photons m^{-2} s^{-1} (12 h:12 h diurnal cycling).

Experimental measurement setup
All amperiometric and potentiometric microsensor measurements were conducted in a self-constructed Faraday cage to minimize electrical disturbance. A detailed description of the measurement setup can be found in Polerecky et al. (2007). Diseased corals fragments were placed in a flow chamber on top of inert sand connected to a circulation system of filtered, aerated natural seawater (1 μm mesh size, 50 l). Seawater conditions were monitored throughout the experiment and kept constant at 26 °C, salinity 35, oxygen saturation of 207.8 ± 0.4 μM (mean ± s.e.), pH (total scale) 8.062 ± 0.005 (mean ± s.e.) and a laminar flow of 1 cm s^{-1}. Illumination was provided and regulated directly from above via a fiber-optic guide from a halogen-light source (Schott KL2500, Mainz, Germany). Light intensities were monitored with a quantum irradiance meter (LI-250A, LI-COR, Lincoln, NE, USA), combined with a light sensor for photosynthetic active radiation (PAR).

Microelectrodes
Clark-type O2 microsensors with a guard cathode (tip diameter ~40 μm, <1 s response time (t_{90}), detection limit 0.05 μM) were constructed and calibrated as previously described (Revsbech and Jørgensen, 1986). Fast responding H_2S sensors (tip diameter ~50 μm, <1 s response time (t_{90}), detection limit 0.1 μM at pH <9) with an internal reference were prepared and used as previously described (Jeroschewski et al., 1996; Kühl et al., 1998). Five-point H_2S calibrations were performed in anoxic, filtered, acidified natural seawater (pH<4) and exhibiting linear responses up to 1000 μM ($R^2 > 0.99$). pH measurements were performed on the total scale, by
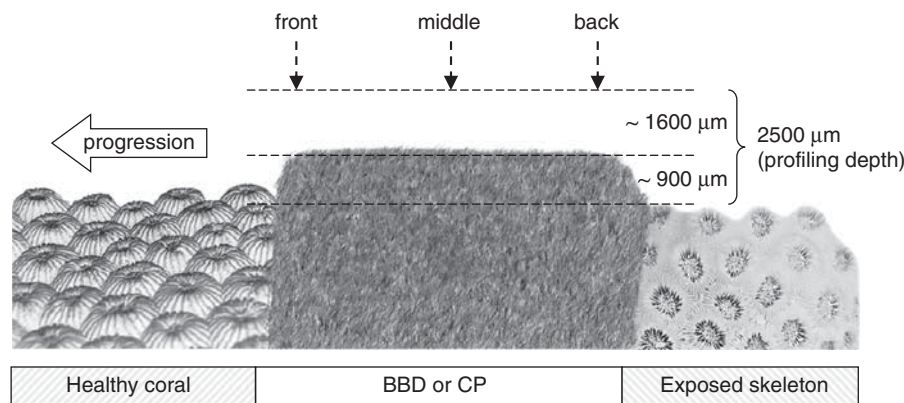
Figure 1 Schematic drawing of profile series conducted for individual disease lesions (CP and BBD). Thickness of microbial mat and profiling depth are exaggerated for clarity.

using liquid ion exchange (LIX) membrane micro-electrodes (tip diameter 20 μm, < 2 s response time (t_{90}), detection limit 0.005) as described by de Beer (2000) and a commercial pH meter (pH 1100, Oakton, Vernon Hills, IL, USA).

Experimental procedure
Measurement series of pH and H_2S profiles were conducted in three locations across both BBD and CP lesions (lesion's front, middle and back, Figure 1) ($n = 3$) and repeated at three different irradiances (0, 40 and 250 μmol photons $m^{-2} s^{-1}$) to simulate *in situ* underwater light levels for night-time, transient light and day-time light regimes. Total sulphide ($S_{tot} = [H_2S] + [HS^-] + [S^{2-}]$) profiles were calculated from aligned values of pH and H_2S profiles as described by Jeroschewski *et al.* (1996) (equations (6) and (7)). The dissociation constant K_1, expressed as pK_1, was corrected for temperature and salinity according to Millero *et al.* (1988) (equation (4)) and Millero and Hershey (1989, equation (22)).

O_2 measurements were carried out at the lesion's front only, following preliminary measurements showing no horizontal gradient of O_2 across BBD and CP mats. Four different irradiances (0, 60, 125, 485 μmol photons $m^{-2} s^{-1}$, Table 1) were selected to estimate peak O_2 evolution at maximal *in situ* light levels (Sato *et al.*, 2009).

To determine the t_{90} value of steady-state signals of the system O_2, pH and H_2S probes were positioned at the mat surface as well as at 400 μm and at 900 μm depth within the mat for ∼40 min. O_2 and H_2S signals (pA) reached > 90% of steady-state signals within 3–7 min, pH values (mV) took 9–13 min. To ensure steady state, light levels were applied > 10 min prior to measurements for O_2 and H_2S, and > 20 min for pH measurements. Microsensor tips were positioned in contact with BBD or CP mat surfaces using a stereo microscope and a 3D-manual micromanipulator (MM33, Maerzhaeuser, Germany). Profiles were conducted perpendicular to the mat surface from ∼1600 μm above and ∼900 μm into the mats covering the diffusive boundary layer (Figure 1).

Mat-migration speed was determined at the end of the experiment (after 48 h) with a digital caliper by measuring band extensions along the migration direction in a 1-cm big strip enclosing the profiling transect ($n = 5$). Developmental stages of lesions were visually classified at the start and end of the experiment on a scale from 1 to 10 (CP 1-5, BBD 6–10) by determining lesion colour, shading, surface structure and density via the stereomicroscope. Immediately after the completion of microsensor measurements, BBD and CP lesions were sampled from coral fragments with sterile forceps and subsequently weighed and preserved for molecular and pigment analyses.

Quantification of sulphate reducers
A quantitative real-time PCR (qPCR) assay targeting the dissimilatory (bi)sulphite reductase (*dsrA*) gene of sulphate-reducing bacteria (SRB) and a qPCR assay targeting the 16S rRNA gene, as detailed in Bourne *et al.* (2011), provided an estimate of SRB populations relative to total bacteria within the sampled mats. The *dsrA* gene was targeted with primers DSR1-F + and DSR-R, adapted from Kondo *et al.* (2008) and Leloup *et al.* (2007), though modified through the use of the TaqMan chemistry and an additional internal probe (DSRtaq (HEX)-5′-CCGATAACRCYGCCGCCGTAACC GA-3′-(TAMARA)), allowing increased specificity and discrimination in quantification of *dsrA* genes within samples (Bourne *et al.*, 2011). Quantification of the bacterial abundance through targeting of the 16S rRNA gene was adapted from Nadkarni *et al.* (2002) and applied the universal primers 331-F (5′-TCCTACGGGAGGCAGCAGT-3′), 797-R (5′-GGAC TACCAGGGTATCTAATCCTGTT-3′), and the probe BacTaq ((6-FAM)-5′-CGTATTACCGCGGCTGCTGG CAC-3′-(TAMARA)), targeting almost all bacterial phyla.

Chlorophyll a concentrations
Chlorophyll *a* (Chl *a*) within the mat samples of CP and BBD was extracted by sonication in 1 ml buffered

Table 1 O_2 concentration (mean ± s.e., µM) measured at the coral–microbial mat interphase (at 0 µm, see Figure 3) of CP and BBD in darkness and at three irradiances

Light ($\mu mol\,photons\,m^{-2}\,s^{-1}$)	CP (n = 3)	BBD (n = 3)
0	23 ± 17	2 ± 2
60	247 ± 28	19 ± 19
125	468 ± 41	80 ± 73
485	1133 ± 19	467 ± 219

Abbreviations: BBD, black band disease; CP, cyanobacterial patch.

methanol (98% methanol, 2% of 0.5 M tetrabutyl ammonium acetate at pH 6.5) on ice. Samples were centrifuged and the supernatant decanted with a pipette before repeating the extraction with 0.8 ml of buffered methanol and combining both extracts. Chl *a* was determined spectrophotometrically (1 cm path length) using the equations detailed in Porra (2002).

Data analyses
Linear regressions between daily mean migration speeds and biogeochemical parameters from the front and base of the microbial mats (S_{tot}, O_2 and pH), relative abundance of SRB, developmental stages and Chl *a* contents were assessed using Pearson product–moment correlation coefficient (R) and a general linear-regression model. Tested values of S_{tot}, O_2 and pH used in the analyses represent daily average values calculated as means from steady-state light (125 and 250 $\mu mol\,photons\,m^{-2}\,s^{-1}$) and dark values from the front and base of the microbial mats. Regression analyses were performed with the statistical analyses software Origin 7.0 (OriginLab Corporation, Northampton, MA, USA).

Results

Biochemical profiles of CP and BBD lesions
CP mats were mostly devoid of H_2S and S_{tot} at all light levels, with the exception of one sample (CP no. 1) where H_2S (~ 1 µM) and S_{tot} (< 42 µM) were observed in dark and at intermediate light levels (Supplementary Figure S1 and Figure 2). In darkness, the base at the progression front of all CP mats was hypoxic (23 ± 17 µM, Table 1), with lower than ambient pH (7.73 ± 0.25, Table 2) and with profiles of decreasing O_2 and pH towards the base of the mat as exemplified in Figure 3. The base at the progression front of the CP mats was supersaturated with respect to O_2 levels $\geqslant 60\,\mu mol\,photons\,m^{-2}\,s^{-1}$ (Table 1). At intermediate light levels (40 µmol photons $m^{-2}\,s^{-1}$), pH at the base of the progression front was still lower than ambient (7.83 ± 0.26), although it was greater (8.61 ± 0.19) than ambient at 250 $\mu mol\,photons\,m^{-2}\,s^{-1}$ (Table 2). At 125 µmol photons $\mu m^{-2}\,s^{-1}$, the front of the CP mats were O_2 supersaturated throughout as exemplified in

Figure 3. At the maximum irradiance level of 485 µmol photons $m^{-2}\,s^{-1}$, O_2 concentrations reached 1133 ± 19 µM at the front and base of the CP mats (Table 1).

The base of BBD microbial mats was anoxic in darkness (Table 1), with lower than ambient pH (Table 2) and high concentrations of H_2S at the progression front (Supplementary Figure S1). Clear vertical gradients of decreasing O_2 and pH were observed in darkness towards the BBD mat surface and of increasing H_2S towards the base (Figure 3). Also, if present, H_2S showed a horizontal gradient with highest H_2S levels at the progression front of the lesion, and lowest at the back at all light levels (Supplementary Figure S1). O_2 supersaturation was observed at 125 µmol photons $m^{-2}\,s^{-1}$ at the BBD mat surface as indicated in Figure 3 and only at 485 µmol photons $m^{-2}\,s^{-1}$ at the base (Table 1).

Calculations of total sulphide in BBD lesions consistently revealed strong vertical and horizontal spatial gradients from front to back of the lesions at all light levels, with large inter-colony variations in maximum H_2S and consequently S_{tot} (Supplementary Figure S1 and Figure 2). In all samples (with the exception of BBD no. 2 at intermediate light levels) sulphide accumulation was highest at the base of the progression front of BBD mats, where coral tissue was freshly covered and undergoing necrosis (Figure 2). Sulphide concentrations varied with light intensity and gradients decreased horizontally in extent with increasing light intensities (Figure 2). S_{tot} was detectable 1000 µm above the microbial mat surface in BBD no. 1 in darkness and still accumulated up to 450 µM at the base of the progression front in daylight (Figure 2).

Overall, in darkness, oxygen was depleted throughout BDD mats, while low concentrations of oxygen were still present towards the base of the CP mats (Table 1 and Figure 3). Levels of pH at the base of the mats, though highly variable, were generally lower in BBD than in CP (Table 2). Compared with CP, BBD displayed a more defined stratification into a lower (coral tissue–microbial mat interphase) anoxic-sulphidic zone and an upper phototrophic zone.

Virulence and microenvironmental correlates
BBD showed greater mean migration speeds (1.41–8.63 mm day^{-1}) than CP (0.01–1.18 mm day^{-1}), indicating an increased virulence of BBD compared with CP (Table 3). Mean migration rates were significantly correlated with developmental stages of the lesion ($P = 0.042$), presence of sulphide ($P = 0.008$) and anoxic conditions ($P = 0.024$) at the base of the progression front (Table 3). Relative quantification of the *dsrA* gene showed that the contribution of SRB to the total bacterial population increased in BBD relative to CP. However, the presence of sulphide followed trends in oxygenation and therefore the biogeochemical condition of the mats, rather
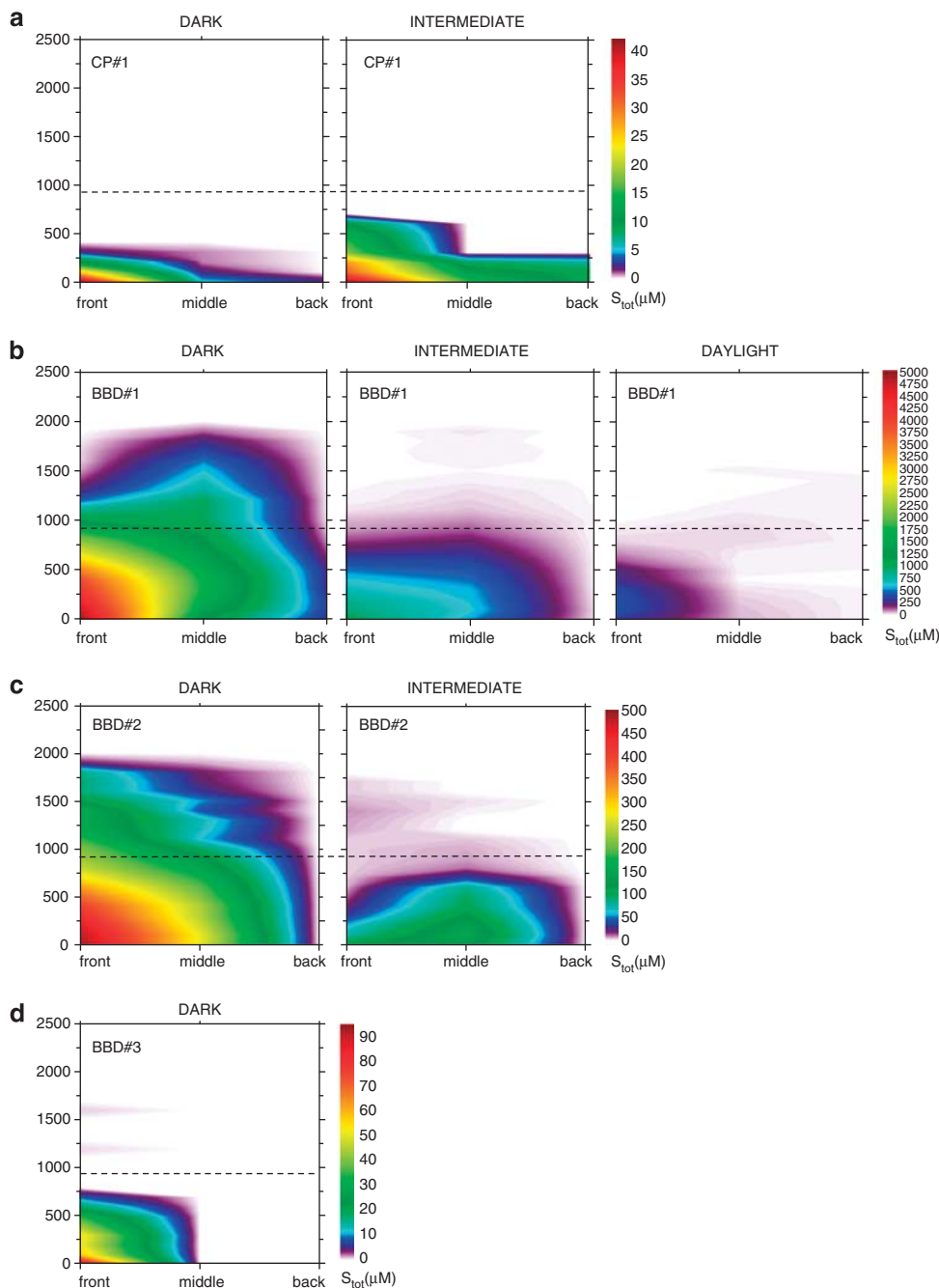
Figure 2 Spatial distribution of total sulphide (S_{tot}) concentrations for (**a**) CP no. 1, (**b**) BBD no. 1, (**c**) BBD no. 2 and (**d**) BBD no. 3 at three different light intensities (darkness = 0, intermediate = 40, daylight = 250 μmol photons $m^{-2} s^{-1}$). Dotted lines indicate the surface of the microbial mats. Scale bars in (**a–d**) are different to allow the representation of S_{tot} in all contour plots. Daylight contour plots for CP no. 1, BBD no. 2, as well as daylight and intermediate contour plots for BBD no. 3 were omitted as they did not contain any sulphide. All contour plots for CP no. 2 and CP no. 3 were also omitted as they did not contain any sulphide.

than the abundance of *dsrA* genes (Table 3). The linear regression analyses showed that mean migration rates were explained better by O_2 and S_{tot} concentrations at the base of the progression front of BBD and CP than by pH and SRB abundance (Table 3). Chl *a* contents also correlated significantly ($P = 0.016$) with migration speeds (Table 3), indicating the presence of high phototrophic biomass within more virulent lesions.

Discussion

Biogeochemistry of BBD and CP microbial mats
The tight coupling of pH, O_2 and total sulphide was characteristic of all disease lesion replicates. It resulted in the development of clearly defined microgradients within the BBD microbial mat, causing a clear stratification into an upper phototrophic (oxygenic) and lower anoxic-sulphidic zone

Table 2 pH (mean ± s.e.) measured at the coral-microbial mat interphase (at 0 μm, see Figure 3) of CP and BBD in darkness and at two irradiances

Light (μmol photons m^{-2} s^{-1})	CP			BBD		
	Front (n = 3)	Middle (n = 3)	Back (n = 3)	Front (n = 3)	Middle (n = 3)	Back (n = 3)
0	7.73 ± 0.25	7.53 ± 0.14	7.75 ± 0.07	7.43 ± 0.20	7.33 ± 0.11	7.49 ± 0.03
40	7.83 ± 0.26	7.74 ± 0.22	7.39 ± 0.23	7.37 ± 0.01	7.62 ± 0.11	7.49 ± 0.19
250	8.61 ± 0.19	8.58 ± 0.22	8.54 ± 0.07	7.58 ± 0.15	8.13 ± 0.27	7.83 ± 0.24

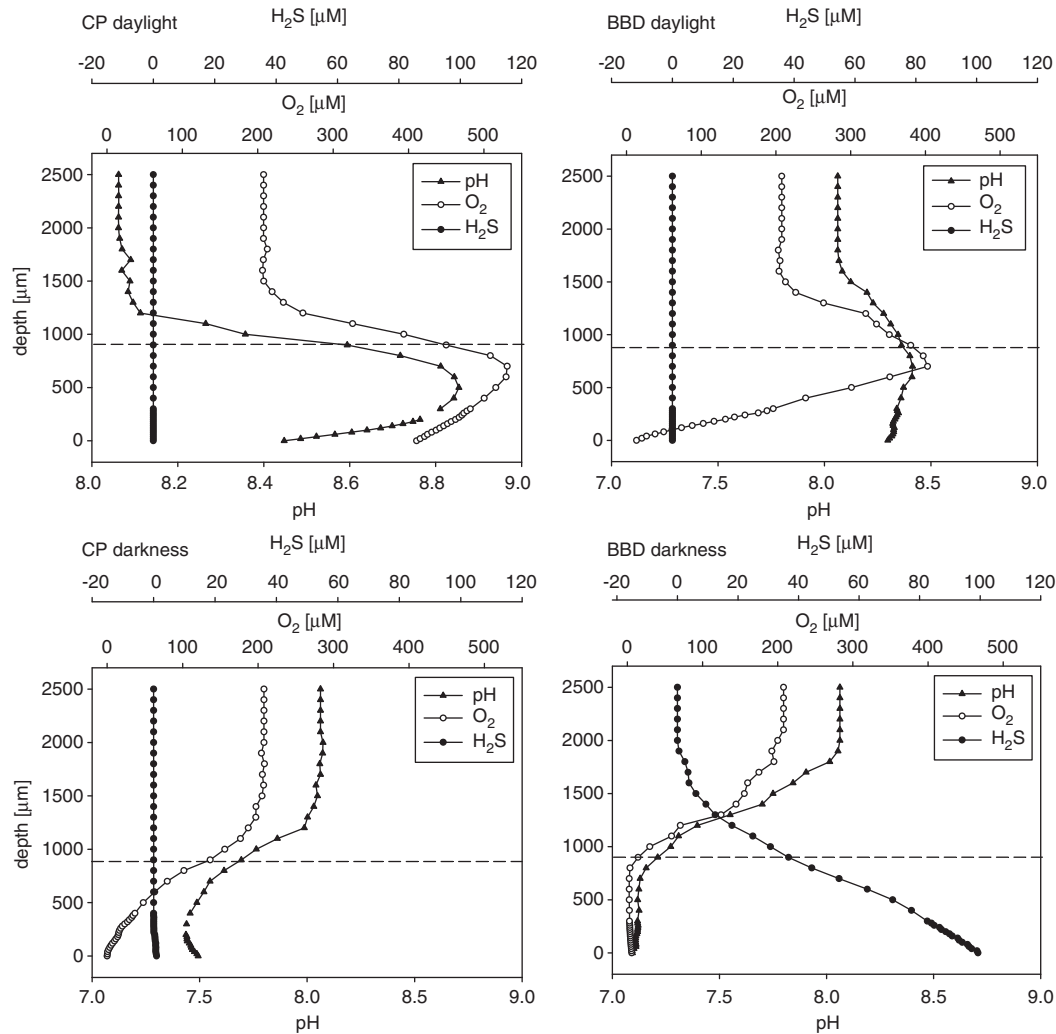Abbreviations: BBD, black band disease; CP, cyanobacterial patch.

Figure 3 Exemplary dark and light profiles of H$_2$S and pH (measured at 250 μmol photons m^{-2} s^{-1}) as well as O$_2$ (measured at 125 μmol photons m^{-2} s^{-1}) at the front of a CP and BBD microbial lesion. The dotted lines indicate the surface of the mats, which were ∼900 μm thick.

in response to varying light levels. These microchemical environments are shaped by the microbial community within the mat, maintaining anoxia, high levels of sulphide and low pH, especially at the coral–microbial mat interphase. Anoxia has been shown to have adverse effects on the photophysiology of endosymbiotic algae (Ulstrup *et al.*, 2005) and overall fitness of the coral host (Shick,

1990). Furthermore, lethal concentrations of sulphide (LC50) on invertebrates (Caldwell, 1975; Bagarinao, 1992; Knezovich *et al.*, 1996; Wang and Chapman, 1999) and coral tissue (Downs *et al.*, 2010) have been reported as low as 0.5 μM for 4 h of exposure, a factor 10^4 lower than the maximum S_{tot} concentrations measured at the base of BBD in this study. This confirms that the measured levels of S_{tot}

Table 3 Mean migration speed, S_{tot}, O_2 and pH measured at the front and base of CP and BBD mats, along with relative quantity of sulphate-reducing bacteria, developmental stages and Chl a contents of individual coral lesions. Results of linear regression analyses are given with respect to migration speed

	Migration speed[a] (mm per day)	Mean S_{tot}[b] (μM)	Mean O_2[b] (μM)	Mean pH[b]	DSR (% per 10^6 16S rRNA)	Developmental stage[c]	Chl a[d] (Chl a g^{-1})
CP no. 1	1.18 ± 0.00	20	193	8.53	2.2	5	80
CP no. 2	0.04 ± 0.01	0	264	7.77	<0.01	2	212
CP no. 3	0.01 ± 0.01	0	278	8.23	0.5	2	313
BBD no. 1	8.63 ± 0.03	2654	0	7.83	9.2	10	733
BBD no. 2	4.19 ± 0.02	246	10	7.22	2.3	9	413
BBD no. 3	1.41 ± 0.02	46	113	7.47	7.8	8	267
Linear regression analyses[e]							
Intercept		1.141	5.976	18.99	0.3354	−2.120	−1.922
Slope		0.003	−0.024	−2.093	0.611	0.783	0.013
R^2		0.856	0.756	0.091	0.505	0.684	0.803
P-value		0.008*	0.024*	0.561	0.113	0.042*	0.016*

Abbreviations: BBD, black band disease; CP, cyanobacterial patch; Chl a, chlorophyll a.
[a]Mean migration speed per day ($n=5$, $\pm$ s.e.).
[b]Mean over light (S_{tot}, pH 250 and O_2 125 μmol photons m^{-2} s^{-1}) and dark conditions.
[c]Developmental stage of lesions assessed by visual inspection.
[d]Stated per wet weight of mats.
[e]Significance levels at the 5% level are indicated by *.

and anoxia in BBD lesions can easily kill coral tissue on short time scales of 1–2 days, during which the microbial mat covers and progresses over the underlying coral tissue. The effects of anoxia and high levels of S_{tot} in BBD drive a high mean migration speed (i.e., virulence) of the lesions, as shown by significant positive linear correlations (Table 3). These deleterious microchemical conditions are established very fast in the dark (t_{90} <10 min; owing to the mats' thinness, which facilitates diffusion), which is in accordance with the fast progression rates of BBD measured in this study *ex situ* (Table 3) and *in situ* (Richardson, 1996; Sato *et al.*, 2009).

In contrast to BBD lesions, the CP microbial mats exhibited no clear vertical stratification into phototrophic-oxygenic and anoxic-sulphidic zones. Consequently, O_2 was present throughout the mat in light (Figure 3), with only a single sample showing marginal sulphide concentrations in the dark and at intermediate irradiances (Figure 2 and Supplementary Figure S1). These conditions resulted in slower mean migration rates and hence lowered virulence of CP compared with BBD measured *ex situ* (Table 3) and *in situ* (Sato *et al.*, 2010).

As both hypoxia and Chl a contents increased with increasing migration speed of all lesions (Table 3), stratification of lesions into photosynthetic and anoxic-sulphidic zones became more pronounced as the lesions developed and virulence increased. This suggests that high cyanobacterial biomass facilitates the biogeochemical stratification as the lesions develop. The results thus show that stratification of the mat community into a phototrophic and anaerobic sulphate reduction zone is essential for the development of anoxia, low pH, high sulphide levels (in darkness) and therefore the increased virulence of BBD compared with CP.

Sulphate reduction and desulphuration in BBD and CP
Both bacterial sulphate reduction and desulphuration of degrading coral tissue and mucus (Hill *et al.*, 1995; Brown and Bythell, 2005) are potential sources of sulphide production at the coral-BBD microbial mat interphase. SRB typically proliferate under anoxic, sulphate-rich conditions made available by degrading tissue of BBD-infected corals. This is consistent with the strongly increased presence of SRB within BBD, representing between ∼2–9% of the bacterial population within the lesions compared with CP (Table 3). In addition to sulphide production by SRB, coral tissue and mucus desulphuration by microbes and remaining coral-derived enzymes is the most likely source of sulphide emergence (Weber, 2009). As sulphate-reduction rates were not measured in this study, distinguishing between the two sources is not feasible. Nevertheless, the BBD mat covering degrading coral tissue will strongly facilitate desulphuration and sulphate reduction and thereby considerably enhance virulence of BBD lesions compared with non-covered degrading coral tissue.

Proposed positive feedback mechanism causing BBD virulence
The stratification of BBD lesions indicates an interaction between the sulphide-tolerant phototrophic cyanobacteria (Myers and Richardson, 2009), SRB and desulphuration. Positive phototaxis in daylight and production of sulphide in darkness (negative chemotaxis) will drive motile cyanobacteria into the upper layer of BBD lesion, thereby creating a positive feedback loop for anoxic conditions at its base. Increased anoxia at the base will facilitate sulphate reduction by SRB and desulphuration and lower sulphide oxidation, which in

turn will drive negative cyanobacterial chemotaxis against increasing sulphide levels. Sulphide production, via chemical oxidation, further facilitates the presence of anoxia and indirectly lower pH, which again will increase disease virulence at the base of the mat. The three synergistic lethal factors (i.e., anoxia, high concentrations of S_{tot} and low pH) thus reciprocally enhance one another at the coral–BBD microbial mat interphase through the feedback mechanisms described above and can thereby easily create a positive feedback loop for disease virulence.

The strong horizontal and vertical gradients of sulphide in the BBD mats are in agreement with the availability of sulphate, which is limited by the presence of necrosed coral tissue at the progression front of the mat, hence its migration direction (Figure 1). The necrosed coral tissue can easily be decomposed through microbial activity (readily available within the mat of BBD) and remaining coral-derived cellular enzymes, resulting in the presence of high concentrations of sulphate. Anaerobic sulphate reduction is therefore proposed to be biogeochemically facilitated at the coral–microbial mat interphase. Desulphuration and the availability of sulphate for SRB are therefore expected to decrease along the migration gradient of the BBD mat, as suggested by the consistently observed equivalent sulphide microgradients (Figure 2). The stronger correlation of migration rates in CP and BBD with S_{tot}, anoxia and Chl *a* contents, rather than relative abundances of *dsrA* copy numbers (Table 3), indicates that the accumulation of S_{tot} by anaerobic sulphate reduction and desulphuration, rather than the presence or abundance of identified pathogenic microbial members, determines the virulence of these diseases.

The findings of this study indicate that the BBD microbial consortium as a whole establishes biogeochemical conditions at the coral–microbial mat interphase that are lethal for coral tissue. By comparing CP with BBD lesions it was shown that stratification of mats into an upper phototrophic and lower anoxic-sulphidic zone is essential for establishing such high disease virulence. The presented findings therefore indicate that steep biogeochemical microgradients, produced and maintained by the entire microbial consortium of BBD, are the major cause for the high virulence of this disease.

Acknowledgements

References

Antonius A. (1973). New observations on coral destruction in reefs. In: *10th Meeting of the Association of Island Marine Laboratories of the Caribbean*, University of Puerto Rico: Association of Island Marine Laboratories of the Caribbean: Mayaguez, Puerto Rico, p 3.

Bagarinao T. (1992). Sulfide as an environmental factor and toxicant: tolerance and adaptations in aquatic organisms. *Aquat Toxicol* **24**: 21–62.

Barneah O, Ben-Dov E, Kramarsky-Winter E, Kushmaro A. (2007). Characterization of black band disease in Red Sea stony corals. *Environ Microbiol* **9**: 1995–2006.

Bourne DG, Muirhead A, Sato Y. (2011). Changes in sulfate-reducing bacterial populations during the onset of black band disease. *ISME J* **5**: 559–564.

Brown BE, Bythell JC. (2005). Perspectives on mucus secretion in reef corals. *Mar Ecol Progr Ser* **296**: 291–309.

Caldwell R. (1975). *Hydrogen Sulfide Effects on Selected Larval and Adult Marine Invertebrates*. Water Resource Research Institute, Oregon State University: Corvallis.

Carlton RG, Richardson LL. (1995). Oxygen and sulfide dynamics in a horizontally migrating cyanobaterial mat: Black band disease of corals. *FEMS Microbiol Ecol* **18**: 155–162.

Cooney RP, Pantos O, Le Tissier MDA, Barer MR, O'Donnell AG, Bythell JC. (2002). Characterization of the bacterial consortium associated with black band disease in coral using molecular microbiological techniques. *Environ Microbiol* **4**: 401–413.

De Beer D. (2000). Potentiometric microsensors for *in situ* measurements in aquatic environments. In: Buffle J, Horvai G (eds). *In Situ Monitoring of Aquatic Systems: Chemical Analysis and Speciation*. Wiley & Sons: London, pp 161–194.

Dillon JG, Miller S, Bebout B, Hullar M, Pinel N, Stahl DA. (2009). Spatial and temporal variability in a stratified hypersaline microbial mat community. *FEMS Microbiol Ecol* **68**: 46–58.

Downs CA, Fauth JE, Downs VD, Ostrander GK. (2010). *In vitro* cell-toxicity screening as an alternative animal model for coral toxicology: effects of heat stress, sulfide, rotenone, cyanide, and cuprous oxide on cell viability and mitochondrial function. *Ecotoxicology* **19**: 171–184.

Dupraz C, Reid RP, Braissant O, Decho AW, Norman RS, Visscher PT. (2009). Processes of carbonate precipitation in modern microbial mats. *Earth-Sci Rev* **96**: 141–162.

Dupraz C, Visscher PT, Baumgartner LK, Reid RP. (2004). Microbe-mineral interactions: early carbonate precipitation in a hypersaline lake (Eleuthera Island, Bahamas). *Sedimentology* **51**: 745–765.

Fourcans A, Sole A, Diestra E, Ranchou-Peyruse A, Esteve I, Caumette P *et al.* (2006). Vertical migration of phototrophic bacterial populations in a hypersaline microbial mat from Salins-de-Giraud (Camargue, France). *FEMS Microbiol Ecol* **57**: 367–377.

Frias-Lopez J, Klaus JS, Bonheyo GT, Fouke BW. (2004). Bacterial community associated with black band disease in corals. *Appl Environ Microbiol* **70**: 5955–5962.

Glas MS, Motti CA, Negri AP, Sato Y, Froscio S, Humpage AR *et al.* (2010). Cyanotoxins are not implicated in the etiology of coral black band disease outbreaks on Pelorus Island, Great Barrier Reef. *FEMS Microbiol Ecol* **73**: 43–54.

Hill RW, Dacey JWH, Krupp DA. (1995). Dimethylsulfoniopropionate in reef corals. *Bull Mar Sci* **57**: 489–494.

Hinck S, Neu TR, Lavik G, Mussmann M, De Beer D, Jonkers HM. (2007). Physiological adaptation of a nitrate-storing beggiatoa sp to diel cycling in a phototrophic hypersaline mat. *Appl Environ Microbiol* **73**: 7013–7022.

Jeroschewski P, Steukart C, Kühl M. (1996). An amperiometric microsensor for the determination of H_2S in aquatic environments. *Anal Chem* **68**: 4351–4357.

Jonkers HM, Ludwig R, De Wit R, Pringault O, Muyzer G, Niemann H *et al.* (2003). Structural and functional analysis of a microbial mat ecosystem from a unique permanent hypersaline inland lake: 'La Salada de Chiprana' (NE Spain). *FEMS Microbiol Ecol* **44**: 175–189.

Knezovich JP, Steichen DJ, Jelinski JA, Anderson SL. (1996). Sulfide tolerance of four marine species used to evaluate sediment and pore-water toxicity. *Bull Environ Contam Toxicol* **57**: 450–457.

Kondo R, Shigematsu K, Butani J. (2008). Rapid enumeration of sulphate-reducing bacteria from aquatic environments using real-time PCR. *Plankton Benthos Res* **3**: 180–183.

Kühl M, Steuchart C, Eickert G, Jeroschewski P. (1998). A H_2S microsensor for profiling biofilms and sediments: application in an acidic lake sediment. *Aquat Microb Ecol* **15**: 201–209.

Leloup J, Loy A, Knab NJ, Borowski C, Wagner M, Jorgensen BB. (2007). Diversity and abundance of sulfate-reducing microorganisms in the sulfate and methane zones of a marine sediment, Black Sea. *Environ Microbiol* **9**: 131–142.

Ludwig R, Al-Horani FA, de Beer D, Jonkers HM. (2005). Photosynthesis-controlled calcification in a hypersaline microbial mat. *Limnol Oceanogr* **50**: 1836–1843.

Millero FJ, Hershey JP. (1989). Thermodynamics and kinetics of hydrogen sulfide in natural waters. *Mar Chem* **18**: 121–147.

Millero FJ, Plese T, Fernandez M. (1988). The dissociation of hydrogen sulfide in seawater. *Limnol Oceanogr* **33**: 269–274.

Myers JL, Richardson LL. (2009). Adaptation of cyanobacteria to the sulfide-rich microenvironment of black band disease of coral. *FEMS Microbiol Ecol* **67**: 242–251.

Nadkarni MA, Martin FE, Jacques NA, Hunter N. (2002). Determination of bacterial load by real-time PCR using a broad-range (universal) probe and primers set. *Microbiology* **148**: 257–266.

Polerecky L, Bachar A, Schoon R, Grinstein M, Jorgensen BB, de Beer D *et al.* (2007). Contribution of Chloroflexus respiration to oxygen cycling in a hypersaline microbial mat from Lake Chiprana, Spain. *Environ Microbiol* **9**: 2007–2024.

Porra RJ. (2002). The chequered history of the development and use of simultaneous equations for the accurate determination of chlorophylls a and b. *Photosynthesis Res* **73**: 149–156.

Revsbech NP, Jørgensen BB. (1986). Microelectrodes: their use in microbial ecology. *Adv Microb Ecol* **9**: 293–352.

Richardson LL. (1996). Horizontal and vertical migration patterns of Phormidium corallyticum and Beggiatoa spp associated with black-band disease of corals. *Microb Ecol* **32**: 323–335.

Richardson LL. (2004). Black band disease. In: Rosenberg E, Loya Y (eds). *Coral Health and Disease*. Springer Berlin: Berlin, Heidelberg, New York, pp 325–349.

Richardson LL, Kuta KG, Schnell S, Carlton RG. (1997). Ecology of the black band disease microbial consortium. *Proceedings of the 8th International Coral Reef Symposium*, Vol. 1. Panama City, Panama, pp 597–600.

Sato Y, Bourne DG, Willis BL. (2009). Dynamics of seasonal outbreaks of black band disease in an assemblage of Montipora species at Pelorus Island (Great Barrier Reef, Australia). *Proc R Soc B Biol Sci* **276**: 2795–2803.

Sato Y, Willis BL, Bourne DG. (2010). Successional changes in bacterial communities during the development of black band disease on the reef coral, Montipora hispida. *ISME J* **4**: 203–214.

Sekar R, Kaczmarsky LT, Richardson LL. (2008). Microbial community composition of black band disease on the coral host Siderastrea siderea from three regions of the wider Caribbean. *Mar Ecol Progr Ser* **362**: 85–98.

Shick JM. (1990). Diffusion limitation and hyperoxic enhancement of oxygen-consumption in zooxanthellate sea-anemones, zoanthids, and corals. *Biol Bull* **179**: 148–158.

Sutherland KP, Porter JW, Torres C. (2004). Disease and immunity in Caribbean and Indo-Pacific zooxanthellate corals. *Mar Ecol Progr Ser* **266**: 273–302.

Ulstrup KE, Hill R, Ralph PJ. (2005). Photosynthetic impact of hypoxia on in hospite zooxanthellae in the scleractinian coral Pocillopora damicornis. *Mar Ecol Progr Ser* **286**: 125–132.

Vismann B. (1991). Sulfide tolerance - physiological-mechanisms and ecological implications. *Ophelia* **34**: 1–27.

Voss JD, Mills DK, Myers JL, Remily ER, Richardson LL. (2007). Black band disease microbial community variation on corals in three regions of the wider Caribbean. *Microb Ecol* **54**: 730–739.

Wang F, Chapman PM. (1999). Biological implications of sulfide in sediment—a review focusing on sediment toxicity. *Environ Toxicol Chem* **18**: 2526–2532.

Weber M. (2009). How sediment damages corals. PhD thesis, University of Bremen, Bremen.

Supplementary Information accompanies the paper on The ISME Journal website (http://www.nature.com/ismej)